

## A decoupling FEM for simulating near-field wave motion in two-phase media

S. L. Chen<sup>†</sup>

*College of Aerospace Engineering, Nanjing University of Aeronautics and Astronautics,  
Nanjing 210016, China*

Z. P. Liao<sup>‡</sup>

*Institute of Engineering Mechanics, China Seismological Bureau, Harbin 150080, China*

J. Chen<sup>‡</sup>

*The State Key Laboratory of Vibration, Shock & Noise, Shanghai Jiao Tong University,  
Shanghai 20030, China*

*(Received November 16, 2004, Revised August 1, 2005, Accepted August 14, 2006)*

**Abstract.** A decoupling technique for simulating near-field wave motions in two-phase media is introduced in this paper. First, an equivalent but direct weighted residual method is presented in this paper to solve boundary value problems more explicitly. We applied the Green's theorem for integration by parts on the equivalent integral statement of the field governing equations and then introduced the Neumann conditions directly. Using this method and considering the precision requirement in wave motion simulation, a lumped-mass FEM for two-phase media with clear physical concepts and convenient implementation is derived. Then, considering the innate attenuation character of the wave in two-phase media, an attenuation parameter is introduced into Liao's Multi-Transmitting Formula (MTF) to simulate the attenuating outgoing wave in two-phase media. At last, two numerical experiments are presented and the numerical results are compared with the analytical ones demonstrating that the lumped-mass FEM and the generalized MTF introduced in this paper have good precision.

**Keywords:** two-phase media; transmitting boundary; near-field wave motion; decoupling technique.

---

### 1. Introduction

In fields such as geophysics, civil engineering, and electromagnetics, problems of the near-field wave motion arise if the explanation of certain kind of wave motion phenomenon in a local region is required and if the effects of the environmental medium must be considered in this explanation. The study of near-field wave motions in two-phase media has great importance in many practical

---

<sup>†</sup> Associate Professor, Corresponding author, E-mail: [iemcsl@yahoo.com.cn](mailto:iemcsl@yahoo.com.cn)

<sup>‡</sup> Professor

problems in geomechanics, seismology, oil exploration, and earthquake engineering. Due to the complexity of the governing differential equations, nonlinearity, and inhomogeneity, it is difficult to solve the problem analytically (Gajo and Mongiovi 1995, Chen 1994, Kim *et al.* 2002). Therefore, many investigators have resorted to numerical solutions (Zienkiewicz and Shiomi 1984, Prevost 1985, Yiagos and Prevost 1991, Sandhu and Hong 1987, Karim *et al.* 2002, Zhao *et al.* 2005, Li *et al.* 2004, Diebels *et al.* 1996, Huang *et al.* 2004).

Theoretically, we can apply domain discretization techniques (i.e., finite element method or finite difference method) combining appropriate artificial boundary conditions to simulate near-field wave motions, but for many practical problems, such as the earthquake response of nuclear power plants and large bridges, the number of spatial degrees of freedom involved in numerical computation is often larger than 10,000, and the number of time steps is also about 10,000 considering the strong ground motion duration and time step requirement for numerical stability. That means analyzing the earthquake response of the large structures one time (one forward computation) by some ordinary methods involves solving at least 10,000 orders equations set 10,000 times. Moreover, the earthquake resistant design and inverse problems require such forward computation many times. This time-consuming computation renders some ordinary numerical methods impractical. Thus, we need to find a numerical method which can simulate the near-field wave motion, not only accurately but also efficiently. Fortunately, over the past 20 years Liao *et al.* (1984, 1996, 1999, 2001) have proposed and developed a decoupling technique that has been proved accurate and efficient through a series of numerical experiments for 2- and 3-dimensional benchmark cases.

The research done by Liao *et al.* focuses almost entirely on one-phase media. Thus, in this paper we will generalize the decoupling numerical method into two-phase media. This paper is organized as follows. In Section 2, the mathematical model for near-field wave motions in two-phase media is described. In Section 3, an equivalent but direct weighted residual method is presented, and a lumped-mass finite element model with clear physical meaning is obtained. In Section 4, time integration procedures are discussed, and an explicit scheme is selected. In Section 5, the artificial boundary for two-phase media is discussed, and an artificial boundary condition is proposed which is local and independent of the model. In Section 6, two numerical experiments which demonstrate the accuracy and efficiency of the proposed procedure are presented. Section 7 is devoted to conclusion.

## 2. Mathematical model

### 2.1 Governing differential equations

The two-phase models were discussed in (Chen 2002) in details. In this paper, we mainly introduce a decoupling technique that is not limited to any specific model, so without loss of generality, the model introduced in (Men 1982) is selected. Its equations are reformulated as follows:

for the solid skeleton

$$\mathbf{L}_s^T \boldsymbol{\sigma}' - (1 - n) \mathbf{L}_w^T P + b(\dot{\mathbf{U}} - \dot{\mathbf{u}}) = (1 - n) \rho_s \ddot{\mathbf{u}} \quad (1)$$

for the pore fluid

$$-n\mathbf{L}_w^T P + b(\dot{\mathbf{u}} - \dot{\mathbf{U}}) = n\rho_w \ddot{\mathbf{U}} \quad (2)$$

Compatibility conditions (assuming that the initial pore pressure and initial volumetric strain are zero):

$$-nP = E_w[ne^w + (1-n)e^s] \quad (3)$$

The isotropic linear elastic constitutive law for solid skeleton is written as

$$\boldsymbol{\sigma}' = \mathbf{D}\mathbf{e} \quad (4)$$

and the relation between strain and displacement is

$$\mathbf{e} = \mathbf{L}_s \mathbf{u} \quad (5)$$

Table 1 Model in details

Model	P-SV wave	Three-dimensional
$\mathbf{u}$	$(u_1, u_2)^T$	$(u_1, u_2, u_3)^T$
$\mathbf{U}$	$(U_1, U_2)^T$	$(U_1, U_2, U_3)^T$
$\mathbf{L}_s$	$\begin{bmatrix} \partial/\partial x_1 & 0 \\ 0 & \partial/\partial x_2 \\ \partial/\partial x_2 & \partial/\partial x_1 \end{bmatrix}$	$\begin{bmatrix} \partial/\partial x_1 & 0 & 0 \\ 0 & \partial/\partial x_2 & 0 \\ 0 & 0 & \partial/\partial x_3 \\ \partial/\partial x_2 & \partial/\partial x_1 & 0 \\ 0 & \partial/\partial x_3 & \partial/\partial x_2 \\ \partial/\partial x_3 & 0 & \partial/\partial x_1 \end{bmatrix}$
$\mathbf{L}_w$	$(\partial/\partial x_1, \partial/\partial x_2)$	$(\partial/\partial x_1, \partial/\partial x_2, \partial/\partial x_3)$
$\mathbf{D}$	$E_s \nu_4 \begin{bmatrix} 1 & \nu_2 & 0 \\ & 1 & 0 \\ & & \nu_2 \end{bmatrix}$	$E_s \nu_4 \begin{bmatrix} 1 & \nu_2 & \nu_2 & 0 & 0 & 0 \\ & 1 & \nu_2 & 0 & 0 & 0 \\ & & 1 & 0 & 0 & 0 \\ & & & \nu_3 & 0 & 0 \\ & & & & \nu_3 & 0 \\ & & & & & \nu_3 \end{bmatrix}$
$\boldsymbol{\sigma}'$	$(\sigma'_{11}, \sigma'_{22}, \sigma'_{12})^T$	$(\sigma'_{11}, \sigma'_{22}, \sigma'_{33}, \sigma'_{12}, \sigma'_{23}, \sigma'_{31})^T$
$\mathbf{e}$	$(e_{11}, e_{22}, e_{12})^T$	$(e_{11}, e_{22}, e_{33}, e_{12}, e_{23}, e_{31})^T$

Notation  $E_s$  is the Young's modulus of solid skeleton,  $\nu$  is the Poisson ratio,  $\mu$  is Lamé constant,  $\nu_1 = (1-\nu)/2$ ,  $\nu_2 = \nu/(1-\nu)$ ,  $\nu_3 = (1-2\nu)/2(1-\nu)$ ,  $\nu_4 = (1-\nu)/((1+\nu)(1-2\nu))$

Table 1 Continued

Model	One-dimensional P wave	One-dimensional S wave	SH wave
$\mathbf{u}$	$u$	$u$	$u_3$
$\mathbf{U}$	$U$	$U$	$U_3$
$\mathbf{L}_s$	$\partial/\partial x$	$\partial/\partial x$	$(\partial/\partial x_1, \partial/\partial x_2)^T$
$\mathbf{L}_w$	$\partial/\partial x$		
$\mathbf{D}$	$E_s$	$\mu$	$\mu \begin{bmatrix} 1 & 0 \\ 0 & 1 \end{bmatrix}$
$\boldsymbol{\sigma}'$	$\boldsymbol{\sigma}'$	$\boldsymbol{\tau}$	$(\sigma'_{31}, \sigma'_{32})^T$
$\mathbf{e}$	$e$	$\gamma$	$(e'_{31}, e'_{32})^T$

$$e^s = \mathbf{L}_w \mathbf{u} \quad (6)$$

$$e^w = \mathbf{L}_w \mathbf{U} \quad (7)$$

where  $\mathbf{L}_s$  and  $\mathbf{L}_w$  are differential operator matrix,  $\boldsymbol{\sigma}'$  and  $P$  are the effective stress and the fluid pressure, respectively,  $\mathbf{U}$  and  $\mathbf{u}$  are the displacements of the fluid and solid skeleton, respectively,  $\rho_s$  and  $\rho_w$  represent the densities of the solid skeleton and fluid, respectively,  $n$  is porosity, and  $b$  is defined as  $b = n^2/k$  where  $k$  is the permeability coefficient of the pore fluid,  $E_w$  is the bulk modulus of the pore fluid,  $e^s$  and  $e^w$  denote the volumetric strains of the solid skeleton and pore fluid, respectively,  $\mathbf{e}$  is the solid strain tensor and  $\mathbf{D}$  is the matrix of material constants. The forms of the  $\mathbf{U}$ ,  $\mathbf{u}$ ,  $\mathbf{L}_s$ ,  $\mathbf{L}_w$ ,  $\boldsymbol{\sigma}'$ ,  $\mathbf{D}$  and  $\mathbf{e}$  for different cases are shown in Table 1.

Substituting Eqs. (3), (4), (5), (6), and (7) into Eqs. (1) and (2) respectively, one obtains equilibrium equations in term of  $\mathbf{U}$  and  $\mathbf{u}$ .

$$\mathbf{L}_s^T \mathbf{D} \mathbf{L}_s \mathbf{u} + \frac{(1-n)}{n} \mathbf{L}_w^T E_w [n \mathbf{L}_w \mathbf{U} + (1-n) \mathbf{L}_w \mathbf{u}] + b(\dot{\mathbf{U}} - \dot{\mathbf{u}}) = (1-n) \rho_s \ddot{\mathbf{u}} \quad (8)$$

$$\mathbf{L}_w^T E_w [n \mathbf{L}_w \mathbf{U} + (1-n) \mathbf{L}_w \mathbf{u}] + b(\dot{\mathbf{u}} - \dot{\mathbf{U}}) = n \rho_w \ddot{\mathbf{U}} \quad (9)$$

## 2.2 Boundary conditions

Three types of boundary conditions on the boundary  $\Gamma$  can be considered.

A. Dirichlet boundary condition

On  $\Gamma_D^s$ :

$$\mathbf{u} - \bar{\mathbf{u}} = \mathbf{0} \quad (10a)$$

on  $\Gamma_D^w$ :

$$\mathbf{U} - \bar{\mathbf{U}} = \mathbf{0} \quad (10b)$$

where  $\bar{\mathbf{u}}$  and  $\bar{\mathbf{U}}$  are the prescribed displacements of solid and fluid phase on the boundary  $\Gamma_D$ , respectively.

B. Neumann boundary condition

On  $\Gamma_N^s$ :

$$\hat{\mathbf{n}}\boldsymbol{\sigma} - \bar{\boldsymbol{\sigma}} = \mathbf{0} \quad (11a)$$

on  $\Gamma_N^w$ :

$$(P - \bar{P})\mathbf{n} = \mathbf{0} \quad (11b)$$

where  $\bar{\boldsymbol{\sigma}}$  and  $\bar{P}$  are the prescribed traction of the solid phase and the pore fluid pressure on the  $\Gamma_N$ , respectively. The vector  $\mathbf{n}$  is the unit outward normal to the boundary  $\Gamma_N$ ,  $\hat{\mathbf{n}}$  is a matrix with unit outward normal components as its elements, and  $\mathbf{n}$  and  $\hat{\mathbf{n}}$  are defined as follows:

$$\mathbf{n} = (n_x, n_y, n_z)^T \quad (12a)$$

$$\hat{\mathbf{n}} = \begin{bmatrix} n_x & 0 & 0 & n_y & 0 & n_z \\ 0 & n_y & 0 & n_x & n_z & 0 \\ 0 & 0 & n_z & 0 & n_y & n_x \end{bmatrix} \quad (12b)$$

C. Artificial boundary conditions

Artificial boundary conditions are needed on the fictitious boundary  $\Gamma_A$  of a finite computational region to model the wave propagation towards infinity. A number of such boundary conditions have been proposed (Degrande and Roeck 1993, Gajo *et al.* 1996, Akiyoshi *et al.* 1998), and the MTF (Liao 1984) is adopted here for its simplicity and local characteristics. The MTF establishes a displacement relation between the nodes on the artificial boundary and nodes in the computation region and can be considered as Dirichlet boundary condition.

The parts  $\Gamma_D^\alpha, \Gamma_N^\alpha (\alpha = s, w)$  and  $\Gamma_A$  of the boundary  $\Gamma$  satisfy the following conditions

$$\Gamma_D^s \cup \Gamma_N^s \cup \Gamma_A = \Gamma \quad \Gamma_D^w \cup \Gamma_N^w \cup \Gamma_A = \Gamma \quad (13a)$$

$$\Gamma_D^s \cap \Gamma_N^s = \mathbf{0} \quad \Gamma_D^s \cap \Gamma_A = \mathbf{0} \quad \Gamma_N^s \cap \Gamma_A = \mathbf{0} \quad (13b)$$

$$\Gamma_D^w \cap \Gamma_N^w = \mathbf{0} \quad \Gamma_D^w \cap \Gamma_A = \mathbf{0} \quad \Gamma_N^w \cap \Gamma_A = \mathbf{0} \quad (13c)$$

### 2.3 Initial conditions

$$\mathbf{u}(\mathbf{x}, 0) = \mathbf{u}_0(\mathbf{x}) \quad \dot{\mathbf{u}}(\mathbf{x}, 0) = \dot{\mathbf{u}}_0(\mathbf{x}) \quad (14a)$$

$$\mathbf{U}(\mathbf{x}, 0) = \mathbf{U}_0(\mathbf{x}) \quad \dot{\mathbf{U}}(\mathbf{x}, 0) = \dot{\mathbf{U}}_0(\mathbf{x}) \quad (14b)$$

### 3. Weak form – Semi-discrete finite element equations

#### 3.1 Weak Galerkin formulation

Given the governing differential equations and initial boundary conditions, the weighted residual method is often used to obtain semi-discrete finite element equations. Here, we perform the method for the above initial boundary value problem.

The satisfaction of Eqs. (8) and (9) is equivalent to the following integral statement:

$$\int_{\Omega} \mathbf{w}_1^T \left( \mathbf{L}_s^T \mathbf{D} \mathbf{L}_s \mathbf{u} + \frac{(1-n)}{n} \mathbf{L}_w^T \mathbf{E}_w [n \mathbf{L}_w \mathbf{U} + (1-n) \mathbf{L}_w \mathbf{u}] \right) dV + \int_{\Omega} \mathbf{w}_1^T (b(\dot{\mathbf{U}} - \dot{\mathbf{u}}) - (1-n) \rho_s \ddot{\mathbf{u}}) dV = 0 \quad (15)$$

$$\int_{\Omega} \mathbf{w}_2^T (\mathbf{L}_w^T \mathbf{E}_w [n \mathbf{L}_w \mathbf{U} + (1-n) \mathbf{L}_w \mathbf{u}] + b(\dot{\mathbf{u}} - \dot{\mathbf{U}}) - n \rho_w \ddot{\mathbf{U}}) dV = 0 \quad (16)$$

where  $\mathbf{w}_1$  and  $\mathbf{w}_2$  are arbitrary weight function vectors.

Discretizing the computation region into nonoverlapping finite elements, the solid skeleton displacement vector  $\mathbf{u}$  and the fluid displacement vector  $\mathbf{U}$  can be approximated as follows:

$$\mathbf{u} = \mathbf{N} \mathbf{u}^e \quad \mathbf{U} = \mathbf{N} \mathbf{U}^e \quad (17)$$

$$\left. \begin{aligned} \mathbf{N} &= [\mathbf{N}_1, \dots, \mathbf{N}_J] \\ \mathbf{N}_j &= N_j(\mathbf{x}) \mathbf{I} \quad j = 1, \dots, J \\ N_j(\mathbf{x}) &= 1, \quad \mathbf{x} = \mathbf{x}_j \\ &= 0 \quad \mathbf{x} = \mathbf{x}_i (i \neq j) \end{aligned} \right\} \quad (18)$$

where  $\mathbf{u}^e$  and  $\mathbf{U}^e$  are the vectors of nodal displacement and  $\mathbf{N}$  is shape function. Here, the same shape functions are used for both the solid and fluid phases.  $J$  is the number of nodes for one element,  $\mathbf{I}$  is  $d \times d$  unit matrix, and  $d$  is the number of the degree of freedom for the solid phase on one node.

Substituting Eq. (17) into Eqs. (15) and (16) and performing the integration on the domain occupied by element  $e$ , one obtains the following:

$$\int_{\Omega^e} \mathbf{w}_1^T \left( \mathbf{L}_s^T \mathbf{D} \mathbf{L}_s \mathbf{N} \mathbf{u}^e + \frac{(1-n)}{n} \mathbf{L}_w^T \mathbf{E}_w [n \mathbf{L}_w \mathbf{N} \mathbf{U}^e + (1-n) \mathbf{L}_w \mathbf{N} \mathbf{u}^e] \right) dV + \int_{\Omega^e} \mathbf{w}_1^T (b(\mathbf{N} \dot{\mathbf{U}}^e - \mathbf{N} \dot{\mathbf{u}}^e) - (1-n) \rho_s \mathbf{N} \ddot{\mathbf{u}}^e) dV = 0 \quad (19)$$

$$\int_{\Omega^e} \mathbf{w}_2^T (\mathbf{L}_w^T \mathbf{E}_w [n \mathbf{L}_w \mathbf{N} \mathbf{U}^e + (1-n) \mathbf{L}_w \mathbf{N} \mathbf{u}^e] + b(\mathbf{N} \dot{\mathbf{u}}^e - \mathbf{N} \dot{\mathbf{U}}^e) - n \rho_w \mathbf{N} \ddot{\mathbf{U}}^e) dV = 0 \quad (20)$$

Applying Green's theorem for integration by parts on the first integral in both Eqs. (19) and (20) and considering the Eqs. (3)-(7), one obtains the following:

$$\begin{aligned}
& - \int_{\Omega^e} \left( (\mathbf{L}_s \mathbf{w}_1)^T \mathbf{D} (\mathbf{L}_s \mathbf{N}) \mathbf{u}^e + \frac{(1-n)}{n} (\mathbf{L}_w \mathbf{w}_1)^T \mathbf{E}_w [n (\mathbf{L}_w \mathbf{N}) \mathbf{U}^e + (1-n) (\mathbf{L}_w \mathbf{N}) \mathbf{u}^e] \right) dV \\
& \quad + \int_{\Omega^e} (\mathbf{w}_1^T b \mathbf{N} (\dot{\mathbf{U}}^e - \dot{\mathbf{u}}^e) - (1-n) \mathbf{w}_1^T \rho_s \mathbf{N} \ddot{\mathbf{u}}^e) dV + \oint_{\Gamma^e} \mathbf{w}_1^T \hat{\mathbf{n}} \boldsymbol{\sigma} d\Gamma = 0 \quad (21)
\end{aligned}$$

$$\begin{aligned}
& - \int_{\Omega^e} \left( (\mathbf{L}_w \mathbf{w}_2)^T \mathbf{E}_w [n (\mathbf{L}_w \mathbf{N}) \mathbf{U}^e + (1-n) (\mathbf{L}_w \mathbf{N}) \mathbf{u}^e] - \mathbf{w}_2^T b \mathbf{N} (\dot{\mathbf{u}}^e - \dot{\mathbf{U}}^e) \right) dV \\
& \quad + \int_{\Omega^e} \mathbf{w}_2^T (-n \rho_w \mathbf{N} \ddot{\mathbf{U}}^e) dV + \oint_{\Gamma^e} \mathbf{w}_2^T \mathbf{n} n P d\Gamma = 0 \quad (22)
\end{aligned}$$

where  $\Omega^e$  is the domain occupied by element  $e$  and  $\Gamma^e$  is the boundary of  $\Omega^e$ .

Substituting Neumann boundary condition (Eq. (11)) into Eqs. (21) and (22), we obtain the following:

$$\begin{aligned}
& - \int_{\Omega^e} \left( (\mathbf{L}_s \mathbf{w}_1)^T \mathbf{D} (\mathbf{L}_s \mathbf{N}) \mathbf{u}^e + \frac{(1-n)}{n} (\mathbf{L}_w \mathbf{w}_1)^T \mathbf{E}_w [n (\mathbf{L}_w \mathbf{N}) \mathbf{U}^e + (1-n) (\mathbf{L}_w \mathbf{N}) \mathbf{u}^e] \right) dV \\
& \quad + \int_{\Omega^e} (\mathbf{w}_1^T b \mathbf{N} (\dot{\mathbf{U}}^e - \dot{\mathbf{u}}^e) - (1-n) \mathbf{w}_1^T \rho_s \mathbf{N} \ddot{\mathbf{u}}^e) dV + \oint_{\Gamma_D^{es} + \Gamma_A^{es}} \mathbf{w}_1^T \hat{\mathbf{n}} \boldsymbol{\sigma} d\Gamma \\
& \quad + \oint_{\Gamma_N^{es}} \mathbf{w}_1^T \bar{\boldsymbol{\sigma}} d\Gamma + \oint_{\Gamma_R^{es}} \mathbf{w}_1^T \hat{\mathbf{n}} \boldsymbol{\sigma} d\Gamma = 0 \quad (23)
\end{aligned}$$

$$\begin{aligned}
& - \int_{\Omega^e} \left( (\mathbf{L}_w \mathbf{w}_2)^T \mathbf{E}_w [n (\mathbf{L}_w \mathbf{N}) \mathbf{U}^e + (1-n) (\mathbf{L}_w \mathbf{N}) \mathbf{u}^e] - \mathbf{w}_2^T b \mathbf{N} (\dot{\mathbf{u}}^e - \dot{\mathbf{U}}^e) \right) dV \\
& \quad + \int_{\Omega^e} \mathbf{w}_2^T (-n \rho_w \mathbf{N} \ddot{\mathbf{U}}^e) dV + \oint_{\Gamma_D^{ew} + \Gamma_A^{ew}} \mathbf{w}_2^T \mathbf{n} n P d\Gamma + \oint_{\Gamma_N^{ew}} \mathbf{w}_2^T \mathbf{n} n \bar{P} d\Gamma \\
& \quad + \oint_{\Gamma_R^{ew}} \mathbf{w}_2^T \mathbf{n} n P d\Gamma = 0 \quad (24)
\end{aligned}$$

where  $\Gamma_R^{e\alpha}, \Gamma_D^{e\alpha}, \Gamma_N^{e\alpha}$  and  $\Gamma_A^{e\alpha}$  ( $\alpha = s, w$ ) are the interface between elements, Dirichlet boundary, Neumann boundary, and artificial boundary parts of  $\Gamma^e$ , respectively. Eqs. (23) and (24) can also be obtained by proceeding along standard procedures (Zienkiewicz and Taylor 1989), that is, the boundary conditions along with the differential equations are written as an equivalent integral formulation with different weight functions ( $\bar{\mathbf{w}}_1, \bar{\mathbf{w}}_2$  for boundary conditions and  $\mathbf{w}_1, \mathbf{w}_2$  for differential equations), then applying Green's theorem for integration by parts and assuming  $\mathbf{w}_1 = -\bar{\mathbf{w}}_1$  and  $\mathbf{w}_2 = -\bar{\mathbf{w}}_2$ , one can obtain Eqs. (23) and (24). Although the above two methods lead to the same results, the way proposed here is more consistent with the way of solving general boundary value problems analytically, that is, first obtaining the general solution of the controlling differential equation, and then combining the boundary conditions to obtain the specific solution. Moreover, the method proposed here need not make the artificial assumption of  $\mathbf{w}_1 = -\bar{\mathbf{w}}_1$  and  $\mathbf{w}_2 = -\bar{\mathbf{w}}_2$ .

As the displacement conditions prescribed on  $\Gamma_D^{e\alpha} + \Gamma_A^{e\alpha}$  can be satisfied in the stage of solving the obtained algebra equations and the weight functions  $\mathbf{w}_1$  and  $\mathbf{w}_2$  are arbitrary, we can ignore the contributions, and then Eqs. (23) and (24) reduce to the following:

$$\begin{aligned}
& - \int_{\Omega^e} \left( (\mathbf{L}_s \mathbf{w}_1)^T \mathbf{D} (\mathbf{L}_s \mathbf{N}) \mathbf{u}^e + \frac{(1-n)}{n} (\mathbf{L}_w \mathbf{w}_1)^T \mathbf{E}_w [n (\mathbf{L}_w \mathbf{N}) \mathbf{U}^e + (1-n) (\mathbf{L}_w \mathbf{N}) \mathbf{u}^e] \right) dV \\
& \quad + \int_{\Omega^e} (\mathbf{w}_1^T b \mathbf{N} (\dot{\mathbf{U}}^e - \dot{\mathbf{u}}^e) - (1-n) \mathbf{w}_1^T \rho_s \mathbf{N} \ddot{\mathbf{u}}^e) dV - \oint_{\Gamma_N^{es}} \mathbf{w}_1^T \bar{\boldsymbol{\sigma}} d\Gamma - \oint_{\Gamma_R^{es}} \mathbf{w}_1^T \hat{\mathbf{n}} \boldsymbol{\sigma} d\Gamma = 0 \quad (25)
\end{aligned}$$

$$\begin{aligned}
& - \int_{\Omega^e} ((\mathbf{L}_w \mathbf{w}_2)^T E_w [n(\mathbf{L}_w \mathbf{N}) \mathbf{U}^e + (1-n)(\mathbf{L}_w \mathbf{N}) \mathbf{u}^e] - \mathbf{w}_2^T b \mathbf{N} (\dot{\mathbf{u}}^e - \dot{\mathbf{U}}^e)) dV \\
& + \int_{\Omega^e} \mathbf{w}_2^T (-n \rho_w \mathbf{N} \ddot{\mathbf{U}}^e) dV + \int_{\Gamma_N^{ew}} \mathbf{w}_2^T \mathbf{n} n \bar{P} d\Gamma + \int_{\Gamma_R^{ew}} \mathbf{w}_2^T \mathbf{n} n P d\Gamma = 0
\end{aligned} \quad (26)$$

For the Galerkin method, the weight functions are selected to be equal to shape functions:

$$\mathbf{w}_1 = \mathbf{N} \quad \mathbf{w}_2 = \mathbf{N} \quad (27)$$

Substituting Eq. (27) into Eqs. (25) and (26), after algebra, one obtains the following:

$$\begin{aligned}
& \int_{\Omega^e} \left( \mathbf{B}_s^T \mathbf{D} \mathbf{B}_s \mathbf{u}^e + \frac{(1-n)}{n} \mathbf{B}_w^T E_w \mathbf{B}_w [n \mathbf{U}^e + (1-n) \mathbf{u}^e] - \mathbf{N}^T b \mathbf{N} (\dot{\mathbf{U}}^e - \dot{\mathbf{u}}^e) \right) dV \\
& + \int_{\Omega^e} ((1-n) \mathbf{N}^T \rho_s \mathbf{N} \ddot{\mathbf{u}}^e) dV - \int_{\Gamma_N^{es}} \mathbf{N}^T \bar{\sigma} d\Gamma - \int_{\Gamma_R^{es}} \mathbf{N}^T \hat{\mathbf{n}} \sigma d\Gamma = 0
\end{aligned} \quad (28)$$

$$\begin{aligned}
& \int_{\Omega^e} (\mathbf{B}_w^T E_w \mathbf{B}_w [n \mathbf{U}^e + (1-n) \mathbf{u}^e] - \mathbf{N}^T b \mathbf{N} (\dot{\mathbf{u}}^e - \dot{\mathbf{U}}^e)) dV \\
& + \int_{\Omega^e} \mathbf{N}^T (n \rho_w \mathbf{N} \ddot{\mathbf{U}}^e) dV + \int_{\Gamma_N^{ew}} \mathbf{N}^T \mathbf{n} n \bar{P} d\Gamma + \int_{\Gamma_R^{ew}} \mathbf{N}^T \mathbf{n} n P d\Gamma = 0
\end{aligned} \quad (29)$$

where

$$\mathbf{B}_s = \mathbf{L}_s \mathbf{N} \quad (30a)$$

$$\mathbf{B}_w = \mathbf{L}_w \mathbf{N} \quad (30b)$$

Eqs. (28) and (29) can be expressed in the matrix form as follows

$$\begin{bmatrix} \mathbf{M}_{ss}^e & \mathbf{0} \\ \mathbf{0} & \mathbf{M}_{ww}^e \end{bmatrix} \begin{pmatrix} \ddot{\mathbf{u}}^e \\ \ddot{\mathbf{U}}^e \end{pmatrix} + \begin{bmatrix} \mathbf{C}_{ss}^e & -\mathbf{C}_{sw}^e \\ -\mathbf{C}_{ws}^e & \mathbf{C}_{ww}^e \end{bmatrix} \begin{pmatrix} \dot{\mathbf{u}}^e \\ \dot{\mathbf{U}}^e \end{pmatrix} + \begin{bmatrix} \mathbf{K}_{ss}^e & \mathbf{K}_{sw}^e \\ \mathbf{K}_{ws}^e & \mathbf{K}_{ww}^e \end{bmatrix} \begin{pmatrix} \mathbf{u}^e \\ \mathbf{U}^e \end{pmatrix} = \begin{pmatrix} \mathbf{F}_s^e + \mathbf{F}_{Rs}^e \\ \mathbf{F}_w^e + \mathbf{F}_{Rw}^e \end{pmatrix} \quad (31)$$

where the element mass matrices are equal to

$$\mathbf{M}_{ss}^e = \int_{\Omega^e} \mathbf{N}^T (1-n) \rho_s \mathbf{N} dV \quad (32)$$

$$\mathbf{M}_{ww}^e = \int_{\Omega^e} \mathbf{N}^T n \rho_w \mathbf{N} dV \quad (33)$$

The element damping matrices, representing the viscous coupling between both phases, are given by

$$\mathbf{C}_{ss}^e = \int_{\Omega^e} \mathbf{N}^T b \mathbf{N} dV \quad (34)$$

From Eqs. (28), (29), and (31), we have

$$\mathbf{C}_{sw}^e = \mathbf{C}_{ws}^e = \mathbf{C}_{ww}^e = \mathbf{C}_{ss}^e \quad (35)$$

The element stiffness matrices are expressed as

$$\mathbf{K}_{ss}^e = \int_{\Omega^e} (\mathbf{B}_s^T \mathbf{D}^s \mathbf{B}_s + \mathbf{B}_w^T (1-n)^2 / n E_w \mathbf{B}_w) dV \quad (36)$$

$$\mathbf{K}_{sw}^e = \int_{\Omega^e} \mathbf{B}_w^T (1-n) E_w \mathbf{B}_w dV \quad (37)$$

$$\mathbf{K}_{ws}^e = \int_{\Omega^e} \mathbf{B}_w^T (1-n) E_w \mathbf{B}_w dV \quad (38)$$

$$\mathbf{K}_{ww}^e = \int_{\Omega^e} \mathbf{B}_w^T n E_w \mathbf{B}_w dV \quad (39)$$

Finally, the external nodal forces are given by

$$\mathbf{F}_s^e = \oint_{\Gamma_N^{es}} \mathbf{N}^T \bar{\boldsymbol{\sigma}}' d\Gamma - \oint_{\Gamma_N^{ew}} \mathbf{N}^T \mathbf{n} (1-n) \bar{P} d\Gamma \quad (40)$$

$$\mathbf{F}_w^e = -\oint_{\Gamma_N^{ew}} \mathbf{N}^T \mathbf{n} n \bar{P} d\Gamma \quad (41)$$

and the mutual forces between elements, which can be canceled in the element assembly process, are expressed as

$$\mathbf{F}_{Rs}^e = \oint_{\Gamma_R^{es}} \mathbf{N}^T \hat{\mathbf{n}} \boldsymbol{\sigma} d\Gamma \quad (42)$$

$$\mathbf{F}_{Rw}^e = -\oint_{\Gamma_R^{ew}} \mathbf{N}^T \mathbf{n} n P d\Gamma \quad (43)$$

### 3.2 Lumped-mass finite element method

Given the element mass matrices, element damping matrices, element stiffness matrices, and the external nodal forces, we can obtain the system equations set for domain  $\Omega$  by assembling these element matrices according to standard procedures (Zienkiewicz and Taylor 1989). This process results in the consistent-mass finite element model. Another finite element model is the lumped-mass model. Although the consistent-mass model is more elegant than the lumped-mass one from a mathematical point of view, the latter has been suggested for use since the decoupling method was first proposed by Liao (1984). The suggestion was based on the following considerations (Liao 1999): (1) the lumped-mass model yields a spatial decoupling scheme, which is substantially more efficient in computation than the spatial coupling scheme resulting from the consistent-mass model; (2) the suggested model is more reasonable in the physical sense that the wave speed must remain finite; (3) the lumped-mass model is not less accurate than the corresponding consistent-mass model as far as the numerical simulation of wave motion in a desired frequency band is concerned; and (4) the restrictions imposed on the time step by the stability criteria for the consistent-mass model are often harsher than those for the lumped-mass one. For the reasons stated above, the lumped-mass model is selected in this study. The lumped-mass model can be obtained by introducing the different shape functions used for the mass matrix from those for the stiffness matrix or by properly selecting

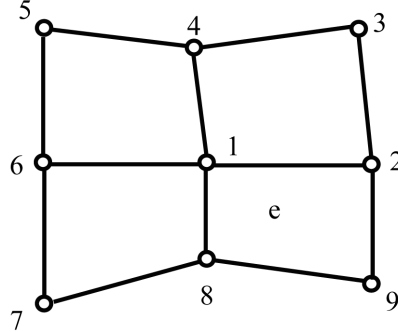


Fig. 1 The local nodal system

the numerical integral points to cause the element not to be on the diagonal zero. Both of them are only from mathematical consideration and lack physical meaning. Here, following the thoughts in Liao (1984) and considering the accuracy requirements for numerical simulation of wave motion, a practical lumped-mass model with clear physical meaning is derived. This model combines the simplicity advantages of the finite difference and the advantages of the finite element method in dealing with inhomogenous medium and irregular boundary.

As we all know, a dynamic disturbance at a spatial point cannot be transmitted to another spatial point instantaneously: it takes time to reach the next point because the wave speed in any realistic medium is finite. In other words, the motion of a specific spatial point at the next moment is determined completely by the motions of its neighboring points in the present and past within a short time window. Therefore, to derive the equations that govern the wave motion of a point, a local nodal system with this point at center is considered. The local nodal system is shown in Fig. 1; the element in the system is quadrilateral and can also be other types.

Assuming the local nodal system consists of  $L$  nodes, the subscript  $(l)$   $l = 1, 2, \dots, L$  denotes the node serial number in this system and the subscript  $j$  denotes the node serial number of a element, there is a relationship between  $l$  and  $j$ , that is,  $l = l(j)$ . So, we have

$$\mathbf{u}_l = \mathbf{u}_{l(j)} = \mathbf{u}_j^e \quad (44a)$$

$$\mathbf{U}_l = \mathbf{U}_{l(j)} = \mathbf{U}_j^e \quad (44b)$$

where  $\mathbf{u}_l$  and  $\mathbf{U}_l$  are the displacement vectors at node  $l$  for solid and fluid phase respectively,  $\mathbf{u}_j^e$  and  $\mathbf{U}_j^e$  are those at node  $j$  for element  $e$ .

Without loss of generality, we assume that node 1 in the system, as shown in Fig. 1, has the same serial number 1 in all elements in this system. According to the physical meaning of elements in stiffness matrix, mass matrix, and damping matrix, i.e., the value of  $K_{ij}$  is equal to that of force imposed on the  $i$ th degree of freedom when unit displacement occurs on the  $j$ th degree of freedom, the equilibrium equations of node 1 can be written as follows:

for the solid phase

$$\sum_e \sum_{j=1}^J (\mathbf{M}_{ss1j}^e \ddot{\mathbf{u}}_j^e + \mathbf{C}_{ss1j}^e \dot{\mathbf{u}}_j^e - \mathbf{C}_{sw1j}^e \dot{\mathbf{U}}_j^e + \mathbf{K}_{ss1j}^e \mathbf{u}_j^e + \mathbf{K}_{sw1j}^e \mathbf{U}_j^e) = \sum_e (\mathbf{F}_{s1}^e + \mathbf{F}_{Rs1}^e) \quad (45)$$

for the fluid phase

$$\sum_e \sum_{j=1}^J (\mathbf{M}_{ww1j}^e \ddot{\mathbf{U}}_j^e - \mathbf{C}_{ws1j}^e \dot{\mathbf{u}}_j^e + \mathbf{C}_{ww1j}^e \dot{\mathbf{U}}_j^e + \mathbf{K}_{ws1j}^e \mathbf{u}_j^e + \mathbf{K}_{ww1j}^e \mathbf{U}_j^e) = \sum_e (\mathbf{F}_{w1}^e + \mathbf{F}_{Rw1}^e) \quad (46)$$

where the first term in Eqs. (45) and (46) is the contribution of inertial forces and other terms on left side are the contribution of constitutive force.  $\mathbf{M}_{aa1j}^e$ ,  $\mathbf{C}_{ab1j}^e$ , and  $\mathbf{K}_{ab1j}^e$  are the  $d \times d$  submatrix of  $\mathbf{M}_{aa}^e$ ,  $\mathbf{C}_{ab}^e$  and  $\mathbf{K}_{ab}^e$ , ( $a, b = s, w$ ), respectively.

To guarantee accuracy in simulating wave motion, the element sizes must be substantially smaller than the smallest wavelength considered. Thus, the spatial variations of acceleration and mass density can be ignored in element region, which means

$$\ddot{\mathbf{u}}_j^e = \ddot{\mathbf{u}}_1 \quad \ddot{\mathbf{U}}_j^e = \ddot{\mathbf{U}}_1 \quad (j = 1, \dots, J) \quad (47)$$

Substituting Eq. (47) into Eqs. (45) and (46) and considering that the mutual forces between elements having the same absolute value but inverse signs, which results in  $\sum_e \mathbf{F}_{Rs1}^e = \sum_e \mathbf{F}_{Rw1}^e = 0$ , the Eqs. (45) and (46) reduce to the following:

$$\ddot{\mathbf{u}}_1 \sum_e \mathbf{M}_{s1}^e + \sum_e \sum_{j=1}^J (\mathbf{C}_{ss1j}^e \dot{\mathbf{u}}_j^e - \mathbf{C}_{sw1j}^e \dot{\mathbf{U}}_j^e + \mathbf{K}_{ss1j}^e \mathbf{u}_j^e + \mathbf{K}_{sw1j}^e \mathbf{U}_j^e) = \sum_e \mathbf{F}_{s1}^e \quad (48)$$

$$\ddot{\mathbf{U}}_1 \sum_e \mathbf{M}_{w1}^e + \sum_e \sum_{j=1}^J (-\mathbf{C}_{ws1j}^e \dot{\mathbf{u}}_j^e + \mathbf{C}_{ww1j}^e \dot{\mathbf{U}}_j^e + \mathbf{K}_{ws1j}^e \mathbf{u}_j^e + \mathbf{K}_{ww1j}^e \mathbf{U}_j^e) = \sum_e \mathbf{F}_{w1}^e \quad (49)$$

where,

$$\mathbf{M}_{s1}^e = \sum_{j=1}^J \mathbf{M}_{ss1j}^e \quad (50)$$

$$\mathbf{M}_{w1}^e = \sum_{j=1}^J \mathbf{M}_{ww1j}^e \quad (51)$$

$\mathbf{M}_{s1}^e$  and  $\mathbf{M}_{w1}^e$  are  $d \times d$  diagonal matrices with the same diagonal elements and the diagonal elements of them denotes the solid and fluid lumped mass on node 1 contributed by element  $e$ , respectively.

The equilibrium equations of other nodes in the computation region (not including the nodes on the artificial boundary) can be derived in the same way as that of node 1. Considering a local nodal system consisting of node  $i$  and its neighboring nodes and assuming that the node with serial number  $k$  of a element corresponds to serial number  $i$  in the system, that is, a relationship of  $k = k(i)$  exists, then the equilibrium equations governing the wave motion of node  $i$  are given as follows:

$$\ddot{\mathbf{u}}_i \mathbf{M}_{si} + \sum_e \sum_{j=1}^J (\mathbf{C}_{ssk(i)j}^e \dot{\mathbf{u}}_j^e - \mathbf{C}_{swk(i)j}^e \dot{\mathbf{U}}_j^e + \mathbf{K}_{ssk(i)j}^e \mathbf{u}_j^e + \mathbf{K}_{swk(i)j}^e \mathbf{U}_j^e) = \sum_e \mathbf{F}_{si}^e \quad (52)$$

$$\ddot{\mathbf{U}}_i \mathbf{M}_{wi} + \sum_e \sum_{j=1}^J (-\mathbf{C}_{wsk(i)j}^e \dot{\mathbf{u}}_j^e + \mathbf{C}_{wwk(i)j}^e \dot{\mathbf{U}}_j^e + \mathbf{K}_{wsk(i)j}^e \mathbf{u}_j^e + \mathbf{K}_{wwk(i)j}^e \mathbf{U}_j^e) = \sum_e \mathbf{F}_{wi}^e \quad (53)$$

where,

$$\mathbf{M}_{si} = \sum_e \mathbf{M}_{sk(i)}^e = \sum_e \sum_{j=1}^J \mathbf{M}_{ssk(i)j}^e \quad (54)$$

$$\mathbf{M}_{wi} = \sum_e \mathbf{M}_{wk(i)}^e = \sum_e \sum_{j=1}^J \mathbf{M}_{wwk(i)j}^e \quad (55)$$

and it can be proven that

$$\mathbf{M}_{sk}^e = \int_{\Omega^e} (1-n) \rho_s \mathbf{N}_k dV \quad (56)$$

$$\mathbf{M}_{wk}^e = \int_{\Omega^e} n \rho_s \mathbf{N}_k dV \quad (57)$$

$$(k = 1, \dots, J)$$

Eqs. (52) and (53) govern the wave motion of inner nodes which refer to all nodes except those on the artificial boundary. The equations that describe the motions of nodes on the artificial will be discussed later.

#### 4. Time integration

Time integration of the semi-discrete finite element Eqs. (52) and (53) can be performed by many types of time stepping algorithms. Broadly speaking, both implicit or explicit procedures are available. Explicit procedures are the most computationally efficient procedures since they do not require (for a lumped-mass model) equation solving to advance the solution, while the implicit procedure require solution of a system of equations at each time step. Although unconditional stability can usually be achieved for implicit procedures, the time step restriction for the whole computation system is determined by the criterion for the stable implementation of the artificial boundary condition, which is comparative to the stability restriction of the explicit procedure. Moreover, the explicit procedure combining the lumped-mass model causes the motion of a specific spatial point at the next moment to be determined completely by the motions of its neighboring points at present and past times within a short time window, which is the character of the wave motion, i.e., local in space and time. Therefore, an explicit procedure is suggested in this study and we select a explicit procedure which results from the combination of the center difference scheme and Newmark scheme (Li *et al.* 1992). After implementation of this explicit scheme in Eqs. (52) and (53), the motions of inner nodes can be expressed as follows:

For displacemen

$$\begin{aligned} \mathbf{u}_i^{p+1} = & -\frac{\Delta t^2}{2} \mathbf{M}_{si}^{-1} \sum_e \sum_{j=1}^J (\mathbf{C}_{ssk(i)j}^e \dot{\mathbf{u}}_j^{ep} - \mathbf{C}_{swk(i)j}^e \dot{\mathbf{U}}_j^{ep} + \mathbf{K}_{ssk(i)j}^e \mathbf{u}_j^{ep} + \mathbf{K}_{swk(i)j}^e \mathbf{U}_j^{ep}) \\ & + \mathbf{u}_i^p + \Delta t \dot{\mathbf{u}}_i^p + \frac{\Delta t^2}{2} \mathbf{M}_{si}^{-1} \sum_e \mathbf{F}_{si}^{ep} \end{aligned} \quad (58a)$$

$$\begin{aligned} \mathbf{U}_i^{p+1} = & -\frac{\Delta t^2}{2} \mathbf{M}_{wi}^{-1} \sum_e \sum_{j=1}^J (-\mathbf{C}_{wsk(i)j}^e \dot{\mathbf{u}}_j^{ep} + \mathbf{C}_{wwk(i)j}^e \dot{\mathbf{U}}_j^{ep} + \mathbf{K}_{wsk(i)j}^e \mathbf{u}_j^{ep} + \mathbf{K}_{wwk(i)j}^e \mathbf{U}_j^{ep}) \\ & + \mathbf{U}_i^p + \Delta t \dot{\mathbf{U}}_i^p + \frac{\Delta t^2}{2} \mathbf{M}_{wi}^{-1} \sum_e \mathbf{F}_{wi}^{ep} \end{aligned} \quad (58b)$$

for velocity

$$\begin{aligned} \dot{\mathbf{u}}_i^{p+1} = & \dot{\mathbf{u}}_i^p - \mathbf{M}_{si}^{-1} \sum_e \sum_{j=1}^J (\mathbf{C}_{ssk(i)j}^e (\mathbf{u}_j^{e(p+1)} - \mathbf{u}_j^{ep}) - \mathbf{C}_{swk(i)j}^e (\mathbf{U}_j^{e(p+1)} - \mathbf{U}_j^{ep})) \\ & + \frac{\Delta t}{2} \mathbf{M}_{si}^{-1} \sum_e \left\{ (\mathbf{F}_{si}^{e(p+1)} + \mathbf{F}_{si}^{ep}) - \sum_{j=1}^J (\mathbf{K}_{ssk(i)j}^e (\mathbf{u}_j^{e(p+1)} + \mathbf{u}_j^{ep}) + \mathbf{K}_{swk(i)j}^e (\mathbf{U}_j^{e(p+1)} + \mathbf{U}_j^{ep})) \right\} \end{aligned} \quad (59a)$$

$$\begin{aligned} \dot{\mathbf{U}}_i^{p+1} = & \dot{\mathbf{U}}_i^p - \mathbf{M}_{wi}^{-1} \sum_e \sum_{j=1}^J (-\mathbf{C}_{wsk(i)j}^e (\mathbf{u}_j^{e(p+1)} - \mathbf{u}_j^{ep}) + \mathbf{C}_{wwk(i)j}^e (\mathbf{U}_j^{e(p+1)} - \mathbf{U}_j^{ep})) \\ & + \frac{\Delta t}{2} \mathbf{M}_{wi}^{-1} \sum_e \left\{ (\mathbf{F}_{wi}^{e(p+1)} + \mathbf{F}_{wi}^{ep}) - \sum_{j=1}^J (\mathbf{K}_{wsk(i)j}^e (\mathbf{u}_j^{e(p+1)} + \mathbf{u}_j^{ep}) + \mathbf{K}_{wwk(i)j}^e (\mathbf{U}_j^{e(p+1)} + \mathbf{U}_j^{ep})) \right\} \end{aligned} \quad (59b)$$

where  $\Delta t$  is the time step,  $\mathbf{u}_i^p$  and  $\mathbf{U}_i^p$  are the displacement vectors of node  $i$  at time  $p\Delta t$  for solid and fluid phase, respectively,  $\mathbf{u}_j^{ep}$  and  $\mathbf{U}_j^{ep}$  are those of node  $j$  for element  $e$  at time  $p\Delta t$ .

## 5. Artificial boundary condition

Some investigators, such as Degrande (1993), Gajo (1996), and Akiyoshi (1998), have studied the artificial boundary for two-phase media. However, the boundary conditions proposed there are almost model dependent or global in time and/or space. Due to their ease of implementation and their local character in space and time domain, local artificial boundary conditions are frequently used for dry elastic media. Among the local artificial boundary conditions, the MTF developed by Liao and his co-workers (Liao 1984) is based solely on a general description of wave propagation and is not geared to any specific system of differential equations that render it general and easy to implement. Considering the attenuation character of wave motion in two-phase media, we have generalized the MTF into the case of two-phase media. For a more detailed derivation, one can refer to (Chen and Liao 2003), and only the final formulas are given below:

$$D\mathbf{u}_0^{p+1} = 0 \quad (60a)$$

$$D\mathbf{U}_0^{p+1} = 0 \quad (60b)$$

$$D = \prod_{m=1}^H (B_0^0 - t_{1,1}^m B_0^1 - t_{1,2}^m \delta_m B_1^1 - t_{1,3}^m (\delta_m)^2 B_2^1) \quad (61)$$

$$\delta_m = \exp(-\beta_{am}\Delta x) \quad (62)$$

$$t_{1,1}^m = (2 - S_m)(1 - S_m)/2 \quad (63a)$$

$$t_{1,2}^m = S_m(2 - S_m) \quad (63b)$$

$$t_{1,3}^m = S_m(S_m - 1)/2 \quad (63c)$$

$$S_m = c_{am}\Delta t/\Delta x \quad (64)$$

Where  $\Delta x$  is the spatial step,  $\mathbf{u}_0^{p+1}$  and  $\mathbf{U}_0^{p+1}$  are the displacement vectors of the artificial boundary point at time  $(p+1)\Delta t$  for solid and fluid phase respectively,  $H$  is the order of the generalized MTF,  $c_{am}$  and  $\beta_{am}$  are the  $m$ th artificial speed and artificial attenuation coefficient, respectively, and  $B_j^q$  is a backward operator with

$$B_j^q \mathbf{u}_n^p = \mathbf{u}_{n+j}^{p-q} \quad (65)$$

where  $\mathbf{u}_n^p$  and  $\mathbf{U}_n^p$  are the displacement vectors at  $x = -n\Delta x$  on the  $x$ -axis, which coincides with the outward normal to the artificial boundary at boundary point 0, with the boundary point 0 as its origin. The formulae (60a) and (60b) are the generalized MTF for attenuation waves in two-phase media, and they can be reduced to the MTF when the attenuation coefficients are zero. Moreover, the generalized MTF is independent of any specific model and local in time and space.

## 6. Numerical examples

Based on the formulae above, we programmed the corresponding finite element codes. Numerical experiments for both two- and three-dimensional cases are presented to verify the accuracy and efficiency of the decoupling procedure.

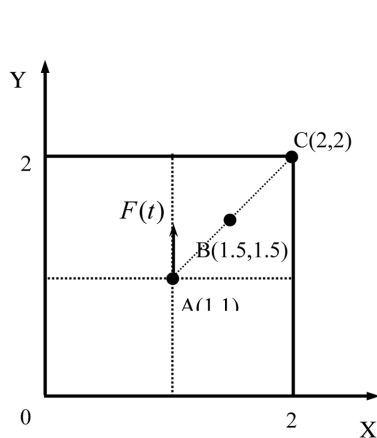


Fig. 2 Two-dimensional point source model in whole space

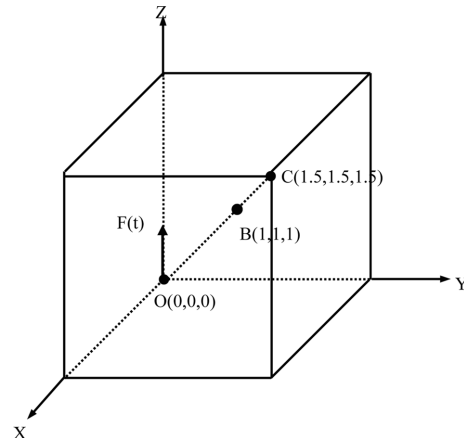


Fig. 3 Three-dimensional point source model in whole space

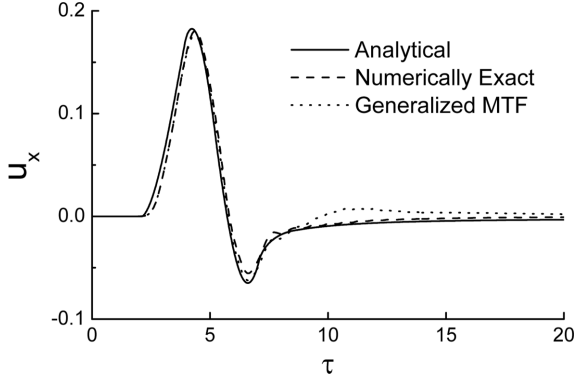


Fig. 4 The displacement of solid phase in  $x$  direction at point (1.5,1.5)

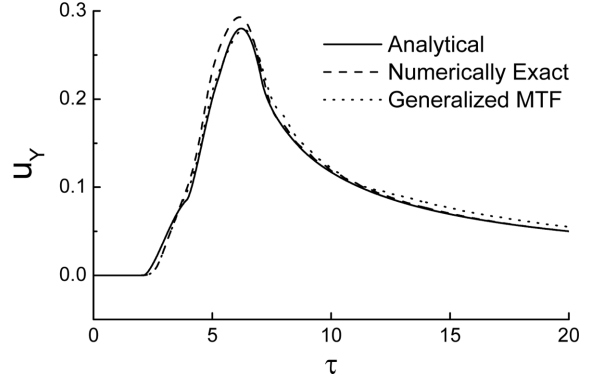


Fig. 5 The displacement of solid phase in  $y$  direction at point (1.5,1.5)

### 6.1 The point source problem in two-dimensional infinite space

Consider a plain strain problem in a two-dimensional infinite domain, as shown in Fig. 2. Suppose that a point force  $F(t)$  acts on the solid skeleton at point (1,1) along  $y$  direction. The function  $F(t)$  is defined as

$$F(t) = \begin{cases} \sin t, & 0 \leq t \leq 1 \\ 0, & t > 1 \end{cases} \quad (66)$$

The non-dimensional parameters used in computation are as follows,  $\lambda = 0.12$ ,  $\mu = 0.24$ ,  $Q = 0.479$ ,  $k = 1.0$ ,  $\rho = 1$ ,  $\rho_w = 0.4$ ,  $m = 2.25$ , and  $\alpha = 1.0$ . Given these parameters, we can obtain the following:  $c_p = 1.0$ ,  $c_d = 0.54$ ,  $c_s = 0.36$ ,  $\eta_p \approx 0.0$ ,  $\eta_d = 0.12$ , and  $\eta_s = 0.013$ , where,  $c_p$ ,  $c_d$ , and  $c_s$  are non-dimensional wave speeds of the fast compressional wave  $P_1$ , the slow compressional wave  $P_2$ , and the shear wave  $S$ , respectively.  $\eta_p$ ,  $\eta_d$  and  $\eta_s$  are the dissipation factors of the above three types of wave, respectively.

The artificial boundaries are placed around the computation region, the dimensions of the model are  $2 \times 2$ , and the computation region is discretized using  $20 \times 20$  four-node square elements, with the nondimensional size  $\Delta x = \Delta y = 0.1$ . The time integration scheme suggested in Section 4 is used with the nondimensional time step  $\Delta t = 0.01$ .

Figs. 4 and 5 depict the solid nondimensional displacements at B(1.5,1.5) in  $x$  and  $y$  directions, respectively, and Figs. 6 and 7 for C (2.0,2.0), with a solid line denoting the analytical solution (Chen 1994), a dash line representing the numerically exact solutions, and a dotted line for the results using generalized MTF. The numerically exact solution means the numerical results with the artificial boundaries placed far enough away that the dynamic behaviors of the regions we were concerned with during the computation time were not affected by the reflected waves from the artificial boundaries. In Figs. 4-7, excellent agreement of the analytical solution and the numerically exact result is seen, which demonstrates that the decoupling technique in this paper has high accuracy. The results using generalized MTF also agree well with the analytical solutions, which tests the accuracy and efficiency of the generalized MTF in simulating the attenuating waves in two-phase media.

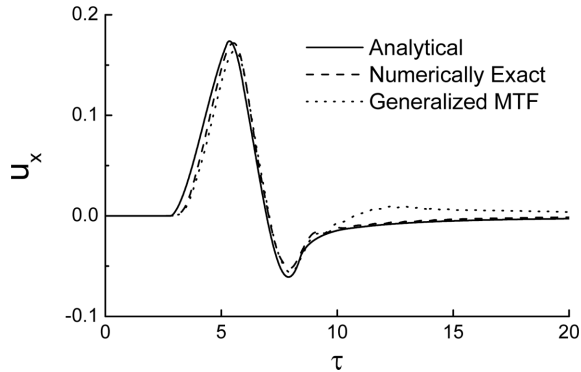


Fig. 6 The displacement of solid phase in  $x$  direction at point  $(2.0,2.0)$

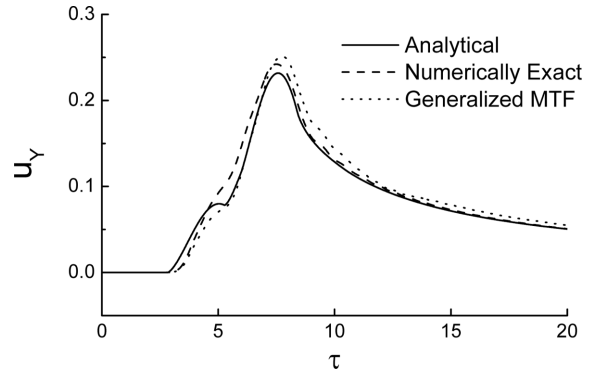


Fig. 7 The displacement of solid phase in  $y$  direction at point  $(2.0,2.0)$

### 6.2 The point source problem in three-dimensional infinite space

Consider a three-dimensional model, as shown in Fig. 3, with artificial boundaries placed on all six surfaces. Suppose that the point force  $F(t)$  (see Eq. (66)) acts on the solid skeleton at point  $(1,1,1)$  along  $z$  direction. The nondimensional parameters are the same as those in the two-dimensional case. The dimensions of the model are  $1.5 \times 1.5 \times 1.5$  and the computation region is discretized using eight-node cubic elements, with the nondimensional size  $\Delta x = \Delta y = \Delta z = 0.1$ . The time integration scheme suggested in Section 4 is used, with the nondimensional time step  $\Delta t = 0.01$ .

Figs. 8 and 9 depict the solid nondimensional displacements at  $B(1.0,1.0,1.0)$  in  $x$  and  $z$  directions, respectively, and Figs. 10 and 11 for  $C(1.5,1.5,1.5)$ , with a solid line denoting analytical solution (Chen 1994), a dash line representing the results using generalized MTF. The displacements in  $y$  direction are the same as those in  $x$  direction for symmetry. The results at boundary node are not as good as those in the two-dimensional case because the boundaries are not far enough away from the source. It is proved in Liao (2001) that the accuracy of the MTF in transmitting more general one-way wave motions may be consistent with that of the finite elements or finite differences in the

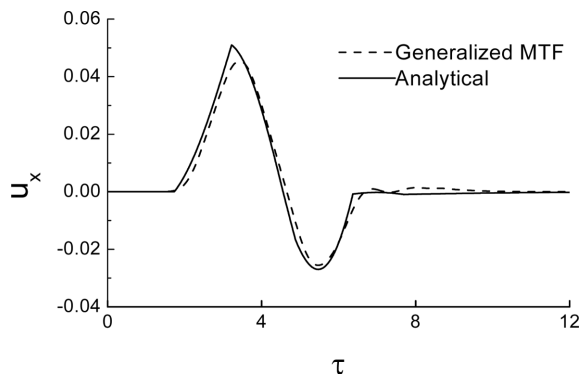


Fig. 8 The displacement of solid phase in  $x$  direction at point  $(1.0,1.0,1.0)$

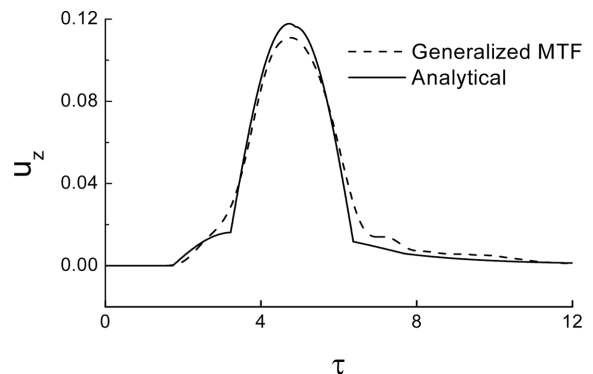


Fig. 9 The displacement of solid phase in  $z$  direction at point  $(1.0,1.0,1.0)$

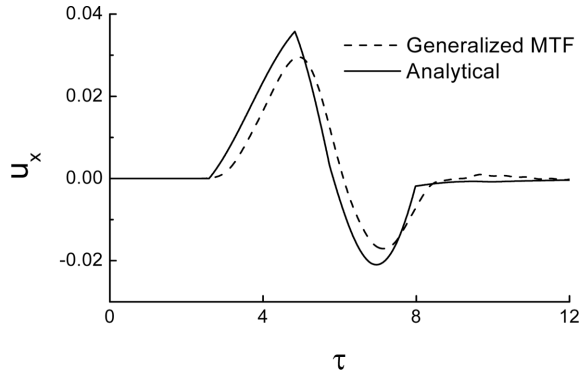


Fig. 10 The displacement of solid phase in x direction at point (1.5,1.5,1.5)

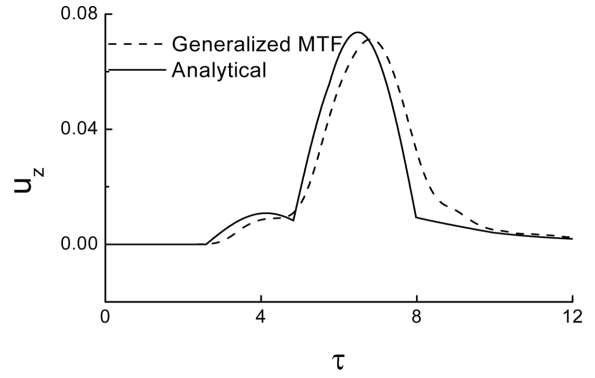


Fig. 11 The displacement of solid phase in z direction at point (1.5,1.5,1.5)

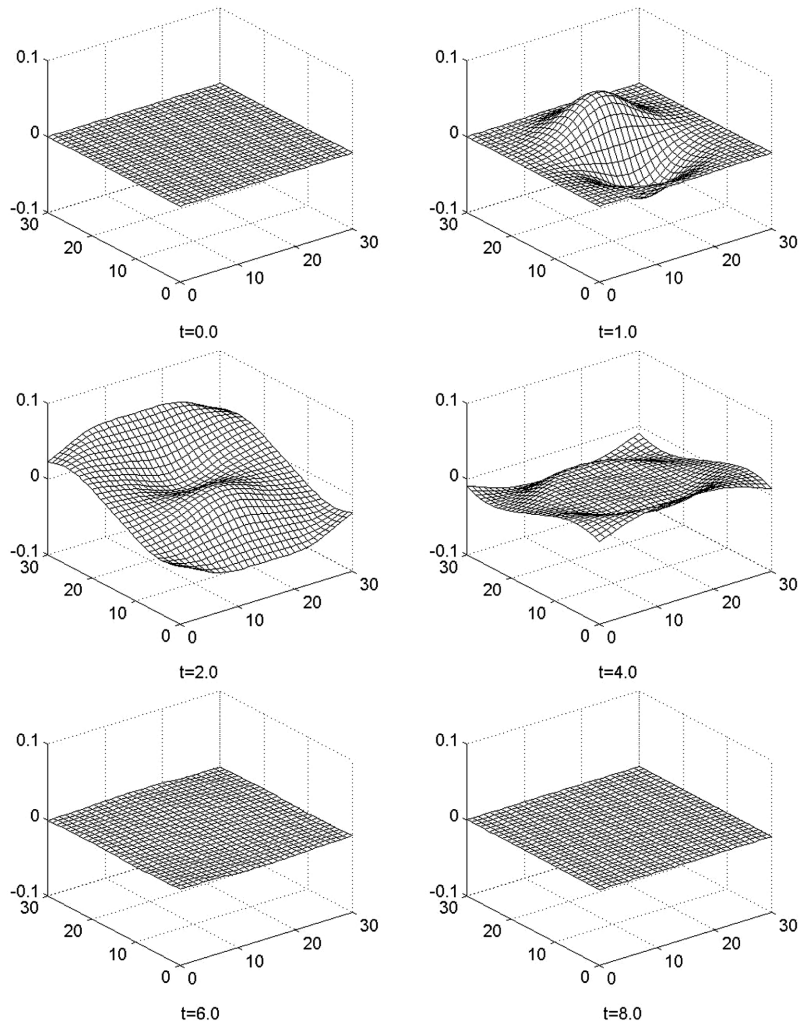


Fig. 12 The snapshot of the solid phase displacement in x direction at  $z = 1.0$

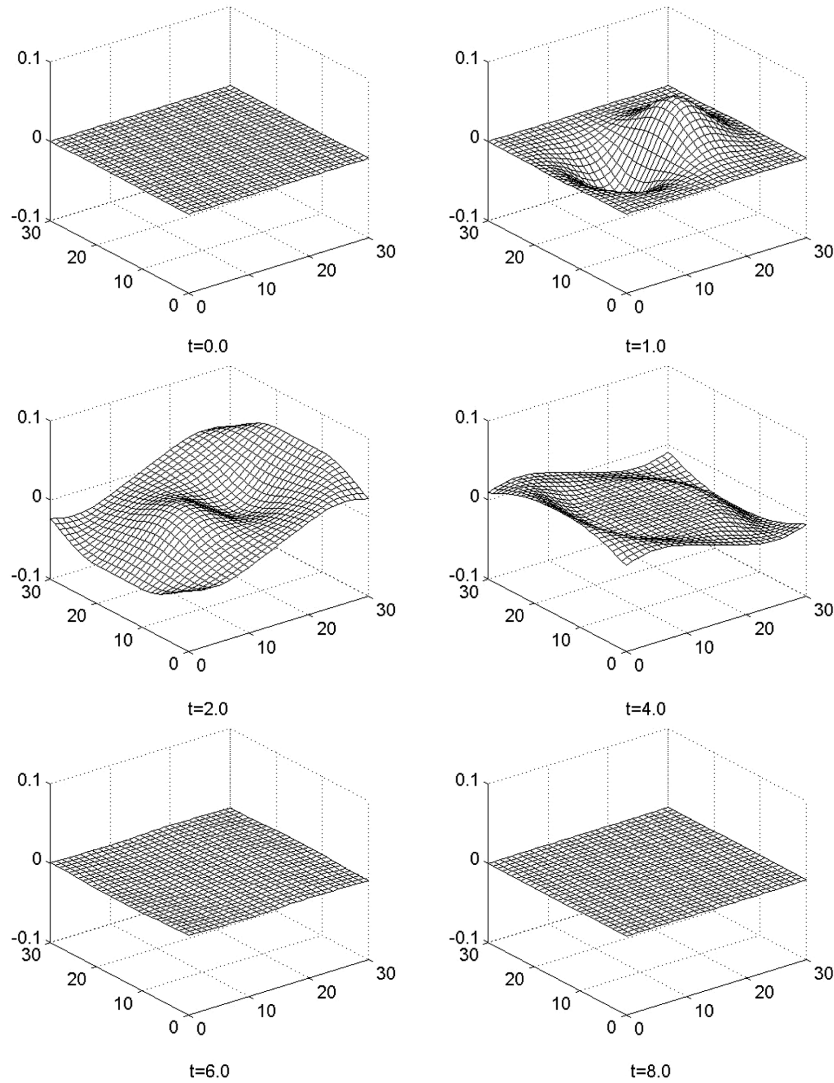


Fig. 13 The snapshot of the solid phase displacement in  $y$  direction at  $z = 1.0$

numerical simulation of wave motion if only the MTF order and the distance between the artificial boundary and the source region are appropriately selected. Figs. 12-14 are the snapshots of solid nondimensional displacements in  $x$ ,  $y$ , and  $z$  directions in transverse section  $z = 1.0$ , respectively.

## 7. Conclusions

The computation is very time-consuming when the problems of near-field wave motion in two-phase media are solved by some ordinary numerical methods, and this renders these methods impractical for engineering. An efficient decoupling technique is presented in this study that consists of the lumped-mass finite element model, explicit time integration procedure, and generalized MTF.

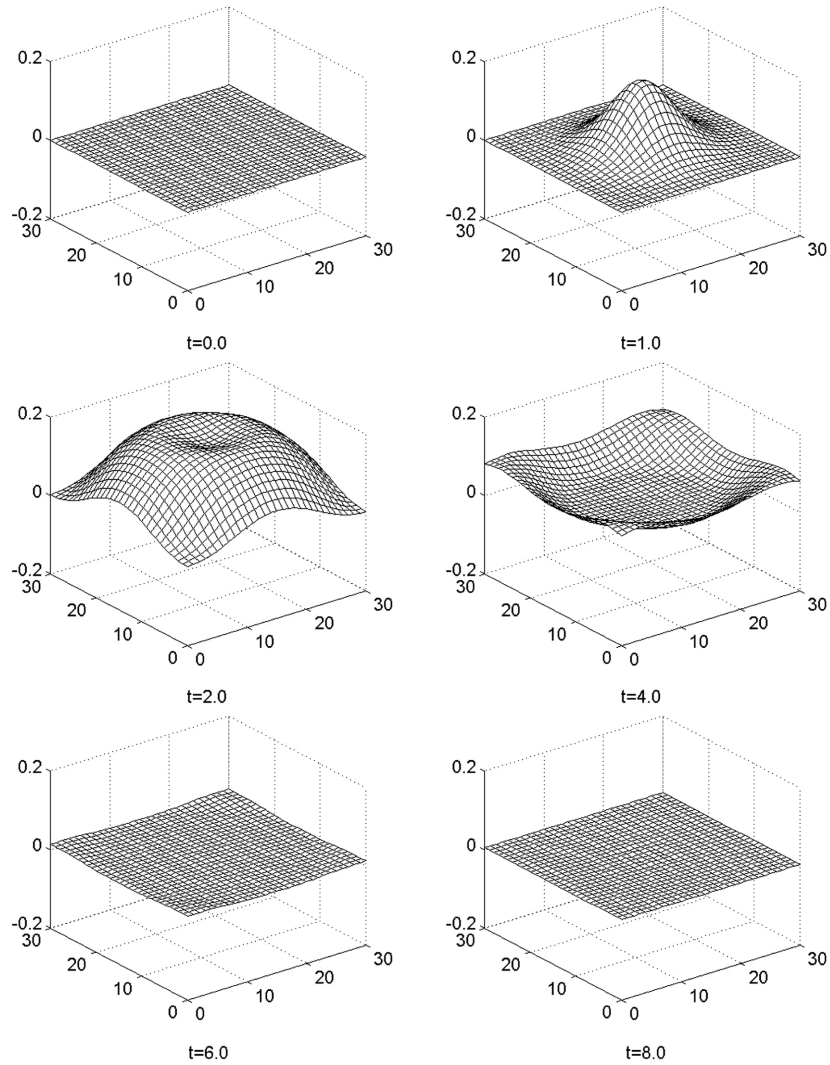


Fig. 14 The snapshot of the solid phase displacement in  $z$  direction at  $z = 1.0$

Meanwhile, an equivalent but direct weighted residual method is presented to solve boundary value problems. Finally, two- and three-dimensional numerical experiments are presented, which test the accuracy and efficiency of the proposed method by comparison with the analytical solutions. We also find the numerical instability in the three-dimensional case. The reason for and the measures to avoid this instability should be studied further.

### Acknowledgments

This study was supported by the Natural Science Foundation of China (50508016). The authors would also like to thank the reviewers for their good suggestions.

## References

- Chen, J. (1994), "Time domain fundamental solution to Biot's complete equations of dynamic poroelasticity, Part I: Two-dimensional solution", *Int. J. Solids Struct.*, **31**(10), 1447-1490.
- Chen, J. (1994), "Time domain fundamental solution to Biot's complete equations of dynamic poroelasticity, Part II: Three-dimensional solution", *Int. J. Solids Struct.*, **31**(2), 169-202.
- Chen, S.L. (2002), "Numerical simulation for near-field wave motion in two-phase media", Ph.D Dissertation, Institute of Engineering Mechanics, China Seismological Bureau, Harbin, China.
- Chen, S.L. and Liao, Z.P. (2003), "Multi-transmitting formula for attenuating waves", *Acta Seismologica Sinica*, **16**(3), 283-291.
- Degrande, G. and Roeck, G.D. (1993), "An absorbing boundary condition for wave propagation in saturated poroelastic media — Part II: Finite element formulation", *Soil Dyn. Earthq. Eng.*, **12**, 423-432.
- Degrande, G. and Roeck, G.D. (1993), "An absorbing boundary condition for wave propagation in saturated poroelastic media—Part I: Formulation and efficiency evaluation", *Soil Dyn. Earthq. Eng.*, **12**, 411-421.
- Diebels, S. and Ehlers, W. (1996), "Dynamic analysis of a fully saturated porous medium accounting for geometrical and material non-linearities", *Int. J. Numer. Meth. Eng.*, **39**(1), 81-97.
- Gajo, A. and Mongioli, L. (1995), "An analytical solution for the transient response of saturated linear elastic porous medium", *Int. J. Numer. Anal. Meth. Geomech.*, **19**, 399-413.
- Gajo, A., Saetta, A. and Vitaliani, R. (1996), "Silent boundary conditions for wave propagation in saturated porous media", *Int. J. Numer. Anal. Meth. Geomech.*, **20**, 253-273.
- Huang, M.S., Yue, Z.Q., Tham, L.G. *et al.* (2004), "On the stable finite element procedures for dynamic problems of saturated porous media", *Int. J. Numer. Meth. Eng.*, **61**(9), 1421-1450.
- Karim, M.R., Nogami, T. and Wang, J.G. (2002), "Analysis of transient response of saturated porous elastic soil under cyclic loading using element-free Galerkin method", *Int. J. Solids Struct.*, **39**, 6011-6033.
- Kim, S.H., Kim, K.J. and Blouin, S.E. (2002), "Analysis of wave propagation in saturated porous media. I. Theoretical solution", *Comput. Meth. Appl. Mech. Eng.*, **191**(37-38), 4061-4073.
- Li, C., Borja, R.I. and Regueiro, R.A. (2004), "Dynamics of porous media at finite strain", *Comput. Meth. Appl. Mech. Eng.*, **193**, 3837-3870.
- Li, X.J., Liao, Z.P. and Du, X.L. (1992), "A explicit integration procedure for dynamic system with damping", *Engineering Mechanics*, Science Press, (in Chinese).
- Liao, Z.P. (1984), "The simulation of near-field wave motion using FEM", *Earthq. Eng. Eng. Vib.*, **2**(1), 1-14, (in Chinese).
- Liao, Z.P. (1996), "Extrapolation non-reflection boundary conditions", *Wave Motion*, **24**(1), 117-138.
- Liao, Z.P. (1999), "Dynamic interaction of natural and man-made structures with earth medium", *Earthq. Res. in China*, **13**(3), 367-408.
- Liao, Z.P. (2001), "Transmitting boundary and radiation conditions at infinity", *Science in China (Series E)*, **44**(2), 177-186.
- Liao, Z.P. and Wong, H.L. (1984), "A transmitting boundary for the numerical simulation of elastic wave propagation", *Soil Dyn. Earthq. Eng.*, **3**(1), 174-183.
- Men, F.L. (1982), "On wave propagation in fluid-saturated porous media", In: *Soil Dynamics and Earthquake Engineering Conference*. Spain, Vol. 1.
- Prevost, J.H. (1985), "Wave propagation in fluid-saturated porous media: An efficient finite element procedure", *Soil Dyn. Earthq. Eng.*, **4**(4), 183-201.
- Sandhu, R.S. and Hong, S.J. (1987), "Dynamics of fluid-saturated soils variational formulation", *Int. J. Numer. Anal. Methods Geomech.*, **11**(1), 241-255.
- Yiagos, A.N. and Prevost, J.H. (1991), "Two-phase elasto-plastic seismic response of earth dams: Application", *Soil Dyn. Earthq. Eng.*, **10**(7), 371-381.
- Zhao, C.G., Li, W.H. and Wang, J.T. (2005), "An explicit finite element method for Biot dynamic formulation in fluid-saturated porous media and its application to a rigid foundation", *J. Sound Vib.*, **282**, 1169-1181.
- Zienkiewicz, O.C. and Shiomi, T. (1984), "Dynamic behaviour of saturated porous media; the generalized biot formulation and its numerical solution", *Int. J. Numer. Meth. Geomech.*, **8**(1), 71-96.
- Zienkiewicz, O.C. and Taylor, R.L. (1989), *The Finite Element Method*, London:McGraw-Hill.